Canadian Conference - Pacific Conference on Earthquake Engineering 2023

Vancouver, British Columbia

June 25th – June 30th, 2023

Sensitivity of the Predicted Lateral Response of UFREIs to Cost Functions For Fitting To Experimental Results

Hediyeh Sheikh[1], Ahmad Alkobari[2], Mirai Jrooj[2], Noor Qarma[2], Rajeev Ruparathna[3], and Niel C. Van Engelen[3*]

[1]PhD Student, Department of Civil and Environmental Engineering, University of Windsor, Ontario, Canada
[2]Undergraduate Student, Department of Civil and Environmental Engineering, University of Windsor, Ontario, Canada
[3]Assistant Professor, Department of Civil and Environmental Engineering, University of Windsor, Ontario, Canada
[*]Niel.VanEngelen@uwindsor.ca (Corresponding Author)

ABSTRACT

The application of fiber-reinforced elastomeric isolators (FREIs) can either be in a bonded or unbonded configuration. The unbonded configuration is particularly advantageous due to the unique rollover deformation that occurs as a result of lateral displacement. This rollover deformation continues until the vertical faces of the isolator contact the supports; a phenomenon referred to as full rollover. This unique behaviour represents a distinct change in the lateral response of unbonded FREIs (UFREIs). Several numerical models have been proposed in the literature that account for the unique hysteresis, each with its own set of assumptions and limitations. However, the calibration of model parameters using experimental data is an essential step to ensure the accuracy of the predictions made by these models. The estimation of the hysteretic behaviour of UFREIs requires the use of appropriate objective functions. This study presents a comparison of objective functions for estimating the best fit to the experimental hysteretic behaviour of UFREIs. The commonly used objective function is entirely based on residual force, which measures the difference between predicted and observed forces at each point of the hysteretic curve. However, the considered objective function is a combination of force and area residuals, which also accounts for the difference between predicted and observed areas under the hysteresis curve. To assess the impact of the objective functions, all possible combinations of their ratios are examined to determine the influence of each on the optimization procedure. The comparison is conducted using the results of previous lateral cyclic and shake table tests performed on a quarter-scale UFREI base isolated structure to determine which combination provides a better estimate of the true force-displacement behaviour of UFREIs. The results suggest that the optimal parameters for numerical models can be determined by minimizing a combination of residual force and area as an objective function.

Keywords: Unbonded fiber-reinforced, objective function, numerical modeling, particle swarm optimization, squared residuals.

INTRODUCTION

Base isolation is a well-established seismic mitigation strategy that has gained significant attention in recent decades for its ability to reduce the vulnerability of structures in regions of moderate to high seismic hazard [1]. The fundamental principle of this approach involves the incorporation of a low stiffness interface between the superstructure and foundation, which serves to dissipate seismic energy and elongate the fundamental period of the structure. The development of effective devices that can provide both a flexible layer and high vertical stiffness has been the subject of research by numerous scholars. The evolution of seismic isolation technology has resulted in the creation of innovative devices, which can generally be classified as either elastomeric or sliding isolators with curved surfaces. Elastomeric isolators rely on the elastic properties of elastomers, which possess a low shear modulus and can accommodate substantial recoverable strains, making them ideal for base isolation. Conversely, sliding isolators utilize low coefficients of friction between two or more surfaces, allowing for sliding movement [2], [3]. The incorporation of reinforcement, either in the form of steel or fibers, in elastomers is required to further improve the vertical and bending properties of the bearing [2]. Fiber-reinforced elastomeric isolators (FREIs) were first proposed by Kelly [4] as a means of reducing the cost and weight-related expenses associated with steel-reinforced elastomeric isolators (SREIs). The resulting device is more suitable for widespread application, particularly in developing countries where the devastation caused by earthquakes is frequently more catastrophic [5].

FREIs can be utilized in both bonded and unbonded configurations between the upper and lower supports. The use of unbonded FREIs (UFREIs) as an alternative to traditional methods of mechanically fastening the isolator to the upper and lower supports has the potential to further improve the performance of these devices [2], [6]. The force-displacement relationship of UFREI displays softening and stiffening regimes due to the rollover effect, which results in an adaptive device with varying characteristics depending on the loading level. The load-displacement relationship under lateral loading can be segmented into three regions: an initial near-linear region, a softening region, and a subsequent stiffening region [7].

Experimental studies conducted on UFREIs demonstrate that both their effective stiffness and equivalent viscous damping exhibit nonlinear behaviour as a function of displacement [8], [9]. In order to accurately assess the seismic response of isolated structures equipped with UFREIs, it is necessary to develop a numerical model that can effectively simulate both the stiffness and damping properties of these isolators [2]. Hysteresis models for UFREIs can be broadly classified into two categories based on the type of equation used to calculate the restoring force: differential models that use differential equations to describe the rate of change of force and displacement (e.g., [10], [11]), and algebraic models that relate force and displacement directly using mathematical equations (e.g., [12]).

The identification of parameters is a challenge in numerical models. Several techniques have been employed in the literature to identify parameters using experimental input and output data, which can be categorized into methods based on minimizing the loss function and those based on nonlinear filtering [13]. The majority of techniques that minimize the loss function aim to minimize a single objective function. However, some studies have explored the impact of incorporating multiple objective functions for Bouc-Wen type models for different structural elements [13], [14]. In the context of isolation systems, the proposed methods for parameter identification are mostly based on minimizing the residual forces [7], [15]–[17].

In this study, particle swarm optimization is utilized to identify the parameters of two leading numerical models of UFREIs, namely the Bouc-Wen model with a fifth-order polynomial [16], [18] and the algebraic model [12]. These models are recognized for their effectiveness in predicting the hysteretic response of UFREIs. The objective function employed in this study takes into account both residual force and residual area. To evaluate the significance of each objective function, the study assigned a weighting coefficient to each one, which helped to consider the impact of each objective function on the optimization process. The comparison is based on the results of previous lateral cyclic and shake table tests that were conducted on a quarter-scale UFREI base-isolated structure [19].

BACKGROUND

Bouc-Wen model

The Bouc-Wen (BW) model, which is a commonly used model for simulating the hysteretic load-displacement behaviour of structural elements, has been extensively studied [16]. The model was first introduced by Bouc [10] and later developed by Wen [11] to offer various hysteretic characteristics. The BW model employs a single nonlinear differential equation to describe a smooth hysteretic behaviour without differentiating between different phases of the applied loading pattern [20]. The horizontal restoring force, F, of the traditional BW model is given by:

$$F = \alpha k_i u + (1-\alpha) u_y k_i z \tag{1}$$

where u_y is the yield displacement, α is the post-yield stiffness ratio, k_i is the initial elastic stiffness, z is the hysteretic parameter, and u is the displacement. The following first-order nonlinear ordinary differential equation is solved to obtain the dimensionless variable z:

$$\dot{z} = \frac{\dot{u}}{u_y}\{A - \gamma|z|^n - \beta \mathrm{sgn}(z\dot{u})|z|^n\} \tag{2}$$

where sgn is the sign function, and A, β, γ, and n are dimensionless parameters that control the shape and size of the hysteresis loop.

Among the numerical models available for UFREIs, Love et al. [18] found that the modified Bouc-Wen (MBW) model, which incorporates a fifth-order polynomial, offers a superior representation of the hysteretic response of UFREIs, particularly at low and intermediate displacement amplitudes. The model is a variation of the traditional Bouc-Wen model and includes a fifth-order polynomial that extends the Chen and Ahmadi [21] version. As a result, the restoring force is modified to:

$$F = a_1 u + a_2|u|u + a_3 u^3 + a_4|u|u^3 + a_5 u^5 + b(1-\alpha)z \tag{3}$$

and the hysteretic parameter is determined from the differential equation:

$$\dot{z} = \frac{\dot{u}}{Y}\{A - \gamma|z|^n - \beta sgn(z\dot{u})|z|^n\} \tag{4}$$

where a_1, a_2, a_3, a_4, and a_5 are stiffness coefficients, and Y replaces u_y in Equation (2). The stiffness coefficients, b, Y, α, β, γ, and n represent the model parameters that need to be calibrated using the results of experimental tests. Note that the coefficient of z in Equation (3), may be absorbed or expanded differently in some references (e.g., [7], [21]). Although viscous damping could also be incorporated in Equation (3), the model used herein only considers hysteretic damping.

Algebraic model

Vaiana et al. [12] introduced an algebraic model for predicting the hysteretic behaviour of UFREIs. The model uses five parameters (k_a, k_b, α, β_1, and β_2), and is based on an algebraic equation for calculating the isolator restoring force. Therefore, it is referred to as the algebraic model (AM). The AM defines a typical force-displacement hysteresis loop using four types of curves: two parallel limiting curves (c_u and c_l), and the loading and unloading curves (c^+ and c). Each parameter of the model affects the size and/or shape of the hysteresis loop. They provided a detailed formulation of the AM and the influence of its parameters on the size and/or shape of the hysteresis loops. To simplify the computer implementation, the authors summarized the procedure in their publication as follows [12]:

1. Initial settings
   1.1. Set the five model parameters: k_a, k_b, α, β_1, and β_2
   1.2. Compute the internal model parameters

$$u_0 = \frac{1}{2}\left[\left(\frac{k_a - k_b}{\delta_k}\right)^{\frac{1}{\alpha}} - 1\right] \tag{5}$$

$$\bar{f} = \frac{k_a - k_b}{2}\left[\frac{(1 + 2u_0)^{(1-\alpha)} - 1}{1 - \alpha}\right] \tag{6}$$

where δ_k can be set to 10^{-20} based on the Vaiana et al. [12] suggestion.

2. Calculations at each time step
   2.1. If $s_t s_{t-\Delta t} < 0$, update the history variable

$$u_j = u_{t-\Delta t} + s_t(1 + 2u_0) - s_t\left\{\frac{s_t(1-\alpha)}{k_a - k_b}\left[f_{t-\Delta t} - \beta_1 u_{t-\Delta t}^3 - \beta_2 u_{t-\Delta t}^5 - k_b u_{t-\Delta t} - s_t\bar{f} + (k_a - k_b)\frac{(1 + 2u_0)^{(1-\alpha)}}{s_t(1-\alpha)}\right]\right\}^{\left(\frac{1}{1-\alpha}\right)} \tag{7}$$

   2.2. Evaluate the restoring force at time t

if $u_j s_t - 2u_0 \leq u_t s_t < u_j s_t$:

$$f_t = \beta_1 u_t^3 + \beta_2 u_t^5 + k_b u_t + (k_a - k_b)\left[\frac{\left(1 + s_t u_t - s_t u_j + 2u_0\right)^{(1-\alpha)}}{s_t(1-\alpha)} - \frac{(1 + 2u_0)^{(1-\alpha)}}{s_t(1-\alpha)}\right] + s_t\bar{f} \tag{8}$$

else:

$$f_t = \beta_1 u_t^3 + \beta_2 u_t^5 + k_b u_t + s_t\bar{f} \tag{9}$$

where s_t is the sign of the velocity at time t (i.e., sgn$(\mathring{u}_t)$), u_t and f_t are displacement and restoring force at time t, respectively, and u_j is a history variable that is updated if the sign of the velocity changes over the time interval.

Particle swarm optimization (PSO)

Particle swarm optimization (PSO) is a nature-inspired optimization algorithm that has been successfully applied in many real-world applications [22]. PSO is a population-based stochastic optimization technique that does not require direct evaluation of gradients, making it suitable for global optimization problems. PSO which was introduced by Kennedy and Eberhart [23], mimics the social behaviour of flocks of birds and swarms of insects and satisfies the five axioms of swarm intelligence: proximity, quality, diverse response, stability, and adaptability [22], [24]. In PSO, particles adjust their trajectories in the design space to search for optimal solutions. Each particle has a position and a velocity, which are updated at each iteration based on its current position and the best positions found by the swarm so far [25]. PSO is a metaheuristic algorithm that can optimize both continuous and discrete problems. There are several variants of PSO, and it can be parallelized to speed up the optimization process [22].

PSO operates on a population of particles, where each particle i (including model parameters) has a position vector x_i and a velocity vector v_i. The position vector x_i represents a potential solution to the optimization problem (i.e., the model parameters), and the velocity vector v_i controls how the particle moves through the search space. The fitness of a particle is evaluated using a fitness function f(x_i) [23].

At each iteration of the algorithm, the particles update their positions and velocities according to the following equations [23]:

$$v_{i(t+1)} = wv_{i(t)} + c_1\text{rand}\left(p_{besti} - x_{i(t)}\right) + c_2\text{rand}\left(g_{besti} - x_{i(t)}\right) \tag{10}$$

$$x_{i(t+1)} = x_{i(t)} + v_{i(t+1)} \tag{11}$$

where t is the current iteration, w is the inertia weight that controls the trade-off between global and local search, c_1 and c_2 are the acceleration coefficients that control the influence of the particle's personal best (p_{best}) and the global best (g_{best}) on the velocity update, rand is a function that generates random values between 0 and 1, and the updates are performed element-wise.

The personal best of particle i, p_{besti}, is the best position that particle i has visited so far. The global best, g_{best}, is the best position visited by any particle in the population. The algorithm terminates when a stopping criterion is met, such as a maximum number of iterations or a satisfactory fitness level. The PSO algorithm can be modified in various ways to improve its performance, such as using different values for the inertia weight, acceleration coefficients, or random values. Additionally, constraints can be added to limit the search space, and multiple swarms can be used to explore different regions of the search space.

METHODOLOGY

In this study, a methodology was developed to evaluate the accuracy of a numerical model for predicting the behaviour of hysteresis loops of the UFREIs under seismic loading. The process of identifying the parameters of numerical models involves least-square optimization in which the difference between the observed response obtained from experiments and the expected response obtained from a computed curve is minimized. By minimizing the residual, or the difference between the observed and expected responses, the optimal values of the parameters can be identified. The objective function can be based on the residual force and residual area of the hysteresis loops to assess the fitness of the numerical model to the experimental data. To account for the effect of both residual force and residual area, the (SS_{res}/SS_{tot}) ratio of R-squared was selected as the objective function to minimize, with a coefficient applied to each term to adjust the weight of each objective. The numerical model parameters were optimized using a numerical optimization algorithm to minimize the objective function. The optimization process involved evaluating various combinations of residual force and residual area coefficients, with increments of 10%, while ensuring that the sum of the coefficients always equaled 1, based on the findings of the experimental cyclic loading test. Then, a time history analysis was conducted on OpenSees software using the same earthquake records that were used in the prior shake table test, and the results are compared with the shake table test results.

The results obtained from the time history analyses for selected different coefficient of objectives are compared with the shake table test results. The comparison includes the hysteresis loops, displacement, force, and acceleration time histories. This comparison enables the evaluation of the accuracy of the numerical model and the effectiveness of the considering residual area as one of the objectives to minimize.

Identification procedure

A two-step optimization procedure is used to identify the nonlinear physical parameters of the Bouc-Wen model. First, polynomial regression is implemented to deduce 5th order polynomial parameters. Second, particle swarm optimization (PSO) is applied for the nonlinear segments to obtain nonlinear physical parameters of a Bouc-Wen hysteretic system. However, since there is no polynomial segment for the AM, only one step optimization using PSO is employed to identify the parameters of the AM. In the MBW model, the constitutive parameters, X, are grouped into two vectors, x_p (parameters related to the polynomial statement) and x_{BW} (parameters for the Bouc-Wen model) as follows:

$$X = \begin{bmatrix} x_p \\ x_{BW} \end{bmatrix}, \qquad x_p = [a_1\ a_2\ a_3\ a_4\ a_5]^T, \qquad x_{BW} = [Y\ b\ \alpha\ \beta\ \gamma]^T \tag{12}$$

where a_1, a_2, a_3, a_4, and a_5 are polynomial coefficients, and Y, b, α, β, and γ are MBW model parameters.

In the AM, the parameters include:

$$X = [x_{AM}], \qquad x_{AM} = [k_a\ k_b\ \alpha\ \beta_1\ \beta_2]^T \tag{13}$$

where k_a, k_b, α, β_1, and β_2 are AM parameters.

Objective function and optimization problem

In this study, the objective is to minimize two objective functions: residual force and residual area. To combine these two objective functions into one, it is crucial to ensure that they are on a comparable scale to give them an adequately weighted importance in the overall optimization process. To achieve this, each objective function must be normalized. The R-squared method is employed in this study to normalize the objective functions to the range from 0 to 1. Once the objective functions have been normalized, they can be combined using a weighted sum, where the weights assigned to each objective function indicate their relative importance in the optimization process. For instance, if residual force is more critical than residual area in a particular case, a higher weight can be assigned to it. The weighted sum of the normalized objective functions yields a single objective function that can be minimized using an optimization algorithm. To evaluate the effects of the two objective functions, all possible combinations of their ratios in increments of 10% are considered to determine how each ratio affects the optimization process.

R-squared is a widely used statistical measure that assesses the goodness-of-fit of a regression model to the data. It is a dimensionless quantity that ranges from 0 to 1 and represents the proportion of the total variation in the actual variable that is explained by the predicted variables in the model. R-squared is formulated as:

$$R^2 = 1 - \left(\frac{SS_{res}}{SS_{tot}}\right) \tag{14}$$

where SS_{res} is the sum of squares of the residuals (the differences between the actual values and the predicted values) and SS_{tot} is the total sum of squares (the differences between the actual values and the mean value of the actual data).

The (SS_{res}/SS_{tot}) fraction was chosen as an appropriate objective function to minimize. This approach ensures that the R-squared value approaches unity, indicating a stronger correlation between the model predictions and experimental data, thereby leading to a better model fit. It is common to use residual force as the objective function to minimize when evaluating the performance of a model in predicting isolation system behaviour. However, in this study, the effect of considering residual area is also evaluated by calculating the (SS_{res}/SS_{tot}) ratio separately. This method enabled an evaluation of the model's effectiveness in terms of both residual force and residual area.

To formulate the optimization problem herein, the (SS_{res}/SS_{tot}) ratio is defined as $R(X)$, where X denotes the set of parameters for the numerical model. To assess the goodness-of-fit of the numerical model, the parameter set X must simultaneously minimize the following two objective functions.

1. The residual sum of squares between the forces measured in the experimental test and the predicted forces with the numerical model:

$$R_1(X) = \frac{\sum_{i=1}^{n}[f(u_i, \dot{u}_i, X) - f^{exp}(u_i)]^2}{\sum_{i=1}^{n}\left[f^{exp}(u_i) - \bar{f}^{exp}\right]^2} \tag{15}$$

where u_i is defined as i-th displacement, f^{exp} is the force value measured at i-th displacement point during the experimental test, f is the predicted force by the numerical model corresponding to the i-th displacement, $\dot{u}_i$ represents i-th velocity, $\bar{f}^{exp}$ is the mean of $f^{exp}(u_i)$, and n is the number of displacement data points obtained from the experimental test.

2. The differences between the area enclosed within each cycle of hysteresis loops calculated from the experimental data and the area enclosed within each cycle of hysteresis loops estimated by numerical model:

$$R_2(X) = \frac{\sum_{j=1}^{m}\left[A_j(X) - A_j^{exp}\right]^2}{\sum_{j=1}^{m}\left[A_j^{exp} - \bar{A}^{exp}\right]^2} \tag{16}$$

where A^{exp} is the area enclosed within each cycle of hysteresis loops calculated from the experimental data, A is the area enclosed within each cycle of hysteresis loops estimated by numerical model, $\bar{A}^{exp}$ is the mean of A_j^{exp}, and m is the number of cycles of the hysteresis loops (i.e., the number of horizontal displacement amplitudes).

To identify the parameters, the following optimization problem needs to be solved:

$$\hat{\theta} = \text{argmin}[R(\theta)|\theta] \tag{17}$$

$$R = \alpha_1 R_1 + \alpha_2 R_2, \quad \alpha_1 + \alpha_2 = 1 \tag{18}$$

$$\alpha = \begin{bmatrix} \alpha_1 \\ \alpha_2 \end{bmatrix}, \theta = \begin{bmatrix} X \\ \alpha \end{bmatrix} \tag{19}$$

where α_1 and α_2 are the weights assigned to each objective function, R is the resulting single objective function that needs to be minimized, and $\hat{\theta}$ represents the set of best solutions returned by PSO algorithm. Note that argmin[R(θ)|θ] denotes the argument θ which minimizes the objective function $R(\theta)$.

RESULTS

To investigate the effect of the considering residual area as one of the objective functions in enhancing the representation of the hysteretic response of UFREIs, numerical model responses with different combination of α_1 and α_2 have been compared against experimental results. The comparison process has been carried out using the outcomes of the previous lateral cyclic testing and shake table testing on a quarter-scale UFREI base isolated structure [19].

Cyclic lateral testing

The results of a quarter-scale UFREI specimen that was experimentally tested by Foster [19], were utilized to investigate the effect of the different value of α_1. The specimen had a square cross-section of 63 mm x 63 mm and a total thickness of elastomeric layers, t_r, of 19.05 mm. The experiment involved subjecting the specimen to three fully reversed sinusoidal cycles at seven different horizontal displacement amplitudes in ascending order, ranging from 0.25 t_r to 2.50 t_r.

To determine the force-displacement hysteresis loops, various sets of parameters were obtained using different values of α_1. Both the MBW model and AM were used to fit the cyclic lateral test results. The effective stiffness, equivalent viscous damping, and area of each cycle were then calculated for all sets of parameters using the method outlined in Ref. [26]. To evaluate the error between the model and experimental data, a weighted average error approach was adopted where the weighting was calculated based on the displacement amplitude of each cycle. This methodology ensured that the importance of each cycle was considered in the calculation, as larger cycles are typically more significant in base isolation systems. Figure 1 and Figure 2 show the weighted average error of the MBW and AM estimation from experimental results at different values of α_1. As expected, the effective stiffness estimation error was reduced when the model parameters were fitted solely based on residual forces (i.e., α_1=100%). However, neglecting the residual area led to higher errors in damping and area.

When α_1 was set to 100%, the error in area was 16.8% in the MBW model and 29.7% in the AM. However, by incorporating the residual area into the objective function with α_1 values ranging from 0% to 90%, the error decreases significantly to a range of 9.18%-10.2% in the MBW model and to a range of 12.7%-17.7% in the AM. The exact error value within this range depends on the specific α_1 value used. Similarly, the error in damping is reduced from 27.9% to a range of 17.0%-21.3% in the MBW model, and from 35.2% to a range of 17.7%-24.7% in the AM, depending on the specific α_1 value used. However, the accuracy of the effective stiffness estimation is negatively affected by the incorporation of the residual area into the objective function. The error in stiffness increases from 13.4% to a range of 14.9%-16.0% in the MBW model, and from 4.80% to a range of 6.55%-9.80% in the AM, indicating a trade-off between the accuracy of the effective stiffness estimation and that of area and damping. Therefore, incorporating the residual area as one of the objective functions can provide a parameter set that better minimizes the objective function. The figures show that the minimum error happens within the range of α_1 values between 0% and 80%, where the area and damping are at their lowest while the stiffness error tolerance remains relatively constant. However, it is recommended to use α_1 values in the range of 10% to 80% to consider a combination of both residual force and area. This is because if the parameters are fitted entirely based on residual area, the results could be meaningless unless the initial values range are close to the actual values. The general trends of the percentage error in the estimation of both numerical models from experimental results at different combinations of α_1 and α_2 are similar, as shown in Figure 1 and Figure 2. The MBW model provided better estimates in terms of area and damping, while the AM provided a better representation of effective stiffness with lower estimation error.

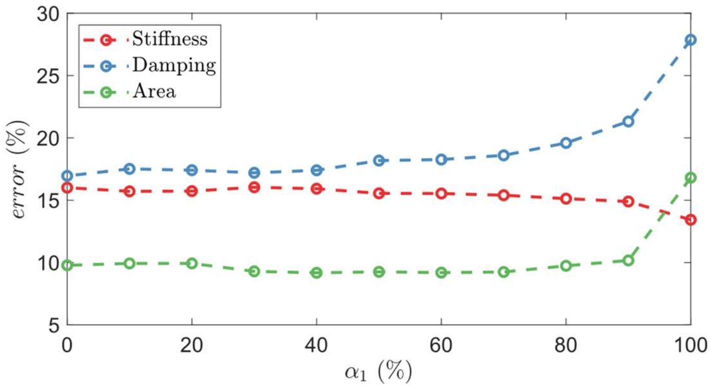

Figure 1. Percent error of the MBW model estimation from experimental results at different combination of α_1 and α_2.

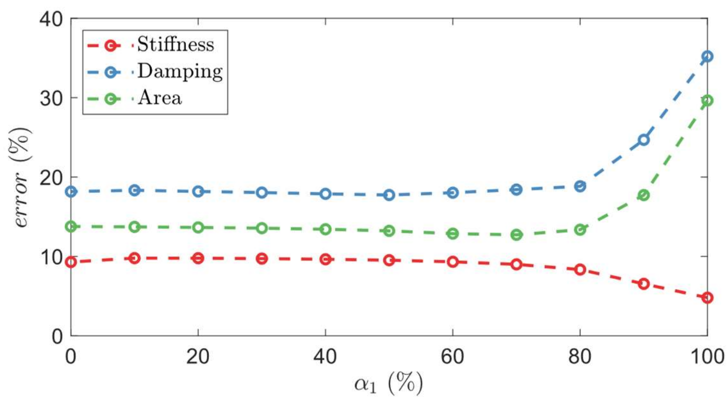

Figure 2. Percent error of the AM estimation from experimental results at different combination of α_1 and α_2.

Time-history analysis

The results of the cyclic lateral tests indicate that the optimal parameters for numerical models can be determined by minimizing a combination of residual force and area as an objective function. To assess the impact of different parameter sets on the response of the structure under time history analysis, two sets of parameters were considered with α_1=100% and α_1=80%. For this purpose, the response of a quarter-scale two-story, single bay moment resisting steel base-isolated structure has been selected from a previous experimental investigation on UFREIs conducted by Foster [19]. Since the shake table testing had been performed on unscragged specimens with the same characteristics as those used in the cyclic loading test, the fitted parameters to the cyclic test with different sets of α_1 can be employed to evaluate the response of the numerical model. In this study, the results of Loma Prieta with 0.3g PGA were used for comparison purposes. The study was conducted in two dimensions using OpenSees software [27]. The beams and columns were modeled using elastic beam-column elements and were assumed to be axially rigid. Figure 3 compares the normalized experimental hysteresis loops of UFREIs under the Loma Prieta 0.3g PGA record and AM responses with α_1=100% and α_1=80% obtained from OpenSees [27]. The running root mean square (RMS) of the displacement, force, and acceleration using a 1-s window were used to compare the estimation error of the models to experimental data, as shown in Figure 4. By calculating the RMS value of each signal during an earthquake event over a sliding window with a specific duration, it is possible to compare signal amplitudes at different times. Although peak values are typically the primary focus, examining the running RMS provides an indication of the overall correspondence across all displacement amplitudes and throughout the event.

To assess the quality of the fit between the experimental and predicted responses, the running RMS of displacement, force, and acceleration were compared, and the absolute differences between them were summed. This was done between a time range of 5s and 20s, excluding data with negligible amplitudes. For the AM with α_1=80%, the sum of the absolute differences for displacement, force, and acceleration responses were 6.04 m, 395 kN, and 47.1 g, respectively. On the other hand, for the AM with α_1=100%, the sum of the absolute differences for displacement, force, and acceleration responses were 12.4 m, 400 kN, and 67.1 g, respectively. These results demonstrate that the AM with α_1=80% provides a better fit to the experimental data than the AM with α_1=100%. Specifically, the AM with α_1=80% fits the experimental data about 100% and 43% better in displacement and acceleration, respectively, compared to the AM with α_1=100%. However, both parameter sets show a relatively similar error in fitting the experimental force data.

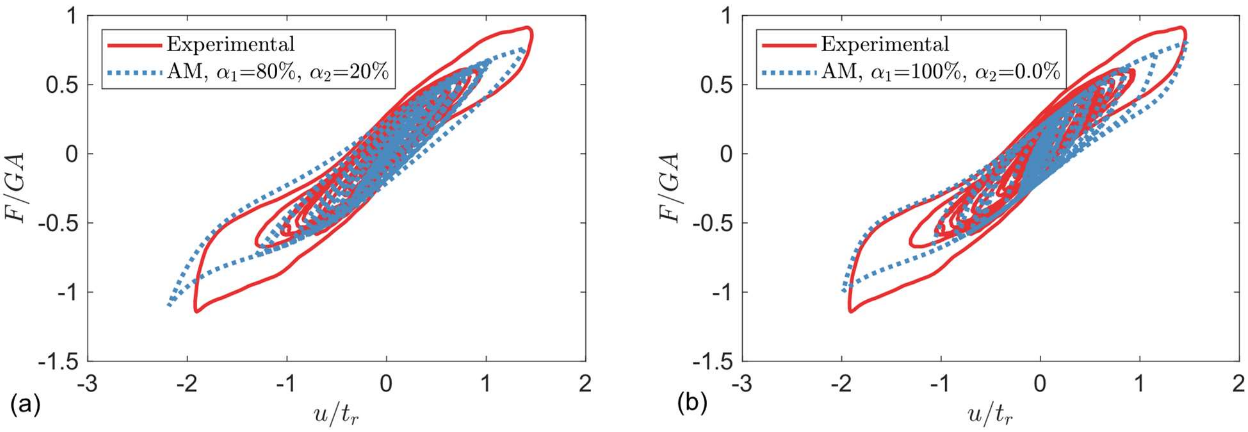

Figure 3. Comparison of the normalized experimental and model hysteretic loops under the Loma Prieta 0.3g PGA record; (a) α_1=80% and (b) α_1=100%.

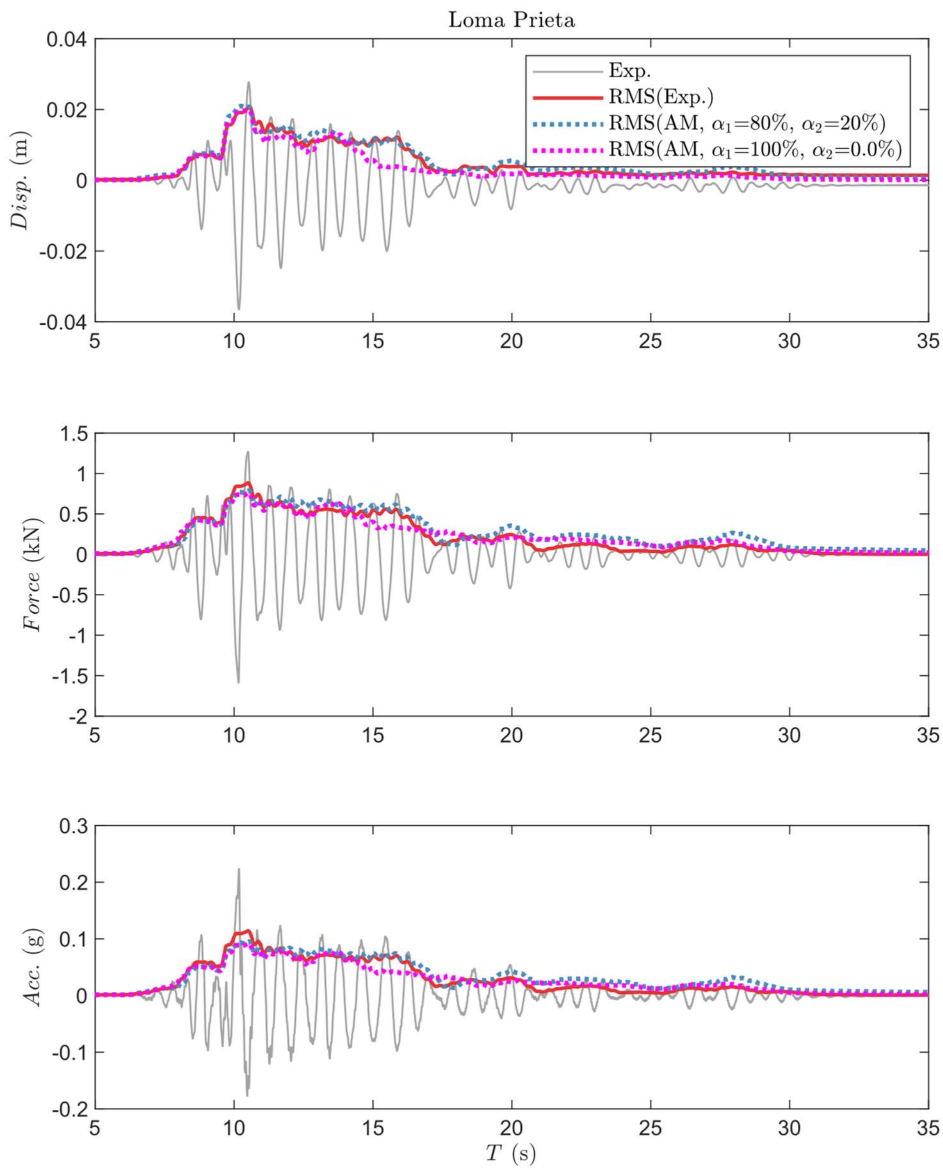

Figure 4. Comparison of the running RMS values obtained using a 1-second window for the experimental and AM responses, with α_1=80% and α_1=100%.

CONCLUSIONS

This study presents a methodology for determining objective functions for fitting numerical models of UFREIs. The methodology incorporates both residual force and residual area as objective functions, with a coefficient applied to each term to adjust the weight of each objective. The optimization process was conducted using cyclic loading test data, and various combinations of residual force and residual area coefficients were applied to minimize the objective function. Next, a time history analysis was conducted using OpenSees software with the parameters derived from the optimization process. Two sets of parameters were evaluated against shake table experimental results. From the analysis, the following conclusions can be drawn:

- The comparison of the predicted and the experimental cyclic loading responses revealed that the inclusion of the residual area in the objective function resulted in a considerable reduction in the average error in both area and damping compared to the case with α_1=100%. The average error in area and damping decreased from 16.8% and 27.9% to a range of 9.18%-10.2% and 17.0%-21.3% in the MBW model, with an increase in effective stiffness error from 13.4% to a range of 14.9%-16.0%. Similar trends were observed in the results obtained by the AM.
- The minimum average error happens within the range of α_1 values between 10% and 80%, where the area and damping are at their lowest while the effective stiffness error remains approximately constant.
- The running RMS of displacement, force, and acceleration were compared to assess the quality of the fit between experimental and predicted responses of a base isolated structure subjected to the Loma Prieta earthquake record. The AM with α_1=80% fits the experimental data about 100% and 43% better in displacement and acceleration, respectively, compared to the AM with α_1=100%. However, both parameter sets exhibit similar errors in fitting the experimental force data.

Note that the results presented in this study are based on one experimental dataset and one seismic record. While the considered methodology and objective function have shown promising results in improving the accuracy of numerical models for UFREIs under seismic loading, further investigations are necessary to verify and control the effectiveness of this approach.

ACKNOWLEDGMENTS

The authors acknowledge the support of the Natural Sciences and Engineering Research Council of Canada (NSERC) [funding reference number RGPIN-2019-03924 and RGPIN-2019-04332]. The undergraduate students were supported by the Undergraduate Research Experience (URE) program at the University of Windsor.

REFERENCES

[1] Clemente, P. (2017). “Seismic isolation: past, present and the importance of SHM for the future,” *J Civ Struct Health Monit*, vol. 7, no. 2, pp. 217–231, doi: 10.1007/s13349-017-0219-6.

[2] Van Engelen, N. C. (2019) “Fiber-reinforced elastomeric isolators: A review,” *Soil Dynamics and Earthquake Engineering*, vol. 125, doi: 10.1016/j.soildyn.2019.03.035.

[3] Becker, T. C., and Mahin, S. A. (2012) “Experimental and analytical study of the bi-directional behavior of the triple friction pendulum isolator,” *Earthq Eng Struct Dyn*, vol. 41, no. 3, pp. 355–373, doi: https://doi.org/10.1002/eqe.1133.

[4] Kelly, J. (1999) “Analysis of Fiber-Reinforced Elastomeric Isolators,” *Journal of Seismology and Earthquake Engineering*, vol. 2, no. 1, pp. 19–34.

[5] Kelly, J. (2002) “Seismic isolation systems for developing countries,” *Earthquake Spectra*, vol. 18, no. 3, pp. 385–406, 2002, doi: 10.1193/1.1503339.

[6] Sheikh, H., Van Engelen, N. C., and Ruparathna, R. (2022) “A review of base isolation systems with adaptive characteristics,” *Structures*, vol. 38, pp. 1542–1555, doi: 10.1016/J.ISTRUC.2022.02.067.

[7] Van Engelen, N. C., Konstantinidis, D., and Tait, M. J. (2016) “Structural and nonstructural performance of a seismically isolated building using stable unbonded fiber-reinforced elastomeric isolators,” *Earthq Eng Struct Dyn*, vol. 45, no. 3, pp. 421–439, doi: 10.1002/EQE.2665.

[8] de Domenico, D., Losanno, D., and Vaiana, N. (2023) “Experimental tests and numerical modeling of full-scale unbonded fiber reinforced elastomeric isolators (UFREIs) under bidirectional excitation,” *Eng Struct*, vol. 274, no. 1, p. 115118, doi: https://doi.org/10.1016/j.engstruct.2022.115118.

[9] Sheikh, H., Ruparathna, R., and Van Engelen, N. C. (2022) “Bi-directional loading of unbonded rectangular fiber-reinforced elastomeric isolators,” *Eng Struct*, vol. 251, p. 113500, Jan. 2022, doi: 10.1016/J.ENGSTRUCT.2021.113500.

[10] Bouc, R. (1967) “Forced vibrations of mechanical systems with hysteresis,” in *Fourth Conference on Nonlinear Oscillations*, Prague: Prague.

[11] Wen, Y.-K. (1976) “Method for random vibration of hysteretic systems,” *Journal of the engineering mechanics division*, vol. 102, no. 2, pp. 249–263, doi: https://doi.org/10.1061/JMCEA3.0002106.

[12] Vaiana, N., Sessa, S., Marmo, F., and Rosati, L. (2019) “An accurate and computationally efficient uniaxial phenomenological model for steel and fiber reinforced elastomeric bearings,” *Compos Struct*, vol. 211, no. 1, pp. 196–212, doi: https://doi.org/10.1016/j.compstruct.2018.12.017.

[13] Ortiz, G., Alvarez, D., and Bedoya-Ruíz, (2013) “Identification of Bouc–Wen type models using multi-objective optimization algorithms,” *Comput Struct*, vol. 114, pp. 121–132.

[14] Li, Z., Noori, M., Zhao, Y., Wan, C., Feng, D., and Altabey, W. A. (2021) “A multi-objective optimization algorithm for Bouc–Wen–Baber–Noori model to identify reinforced concrete columns failing in different modes,” *Proceedings of the Institution of Mechanical Engineers, Part L: Journal of Materials: Design and Applications*, vol. 235, no. 9, pp. 2165–2182. doi: 10.1177/14644207211020028.

[15] Xu, C., Chase, J., and Rodgers, G. (2014) “Physical parameter identification of nonlinear base-isolated buildings using seismic response data,” *Comput Struct*, vol. 145, pp. 47–57.

[16] Manzoori, A., and Toopchi-Nezhad, H. (2017) “Application of an extended Bouc-Wen model in seismic response prediction of unbonded fiber-reinforced isolators,” *Journal of Earthquake Engineering*, vol. 21, no. 1, pp. 87–104, doi: 10.1080/13632469.2016.1138166.

[17] Sessa, S., Vaiana, N., Paradiso, M., and Rosati, L. (2020) “An inverse identification strategy for the mechanical parameters of a phenomenological hysteretic constitutive model,” *Mech Syst Signal Process*, vol. 139, p. 106622.

[18] Love, J., Tait, M., and Toopchi-Nezhad, H. (2011) “A hybrid structural control system using a tuned liquid damper to reduce the wind induced motion of a base isolated structure,” *Eng Struct*, vol. 33, no. 3, pp. 738–746.

[19] Foster, B. A. D. (2012) “Base isolation using stable unbonded fibre reinforced elastomeric isolators (SU-FREI),” McMaster University, Hamilton, Ontario.

[20] Ikhouane, F., and Rodellar, J. (2007) *Systems with hysteresis: analysis, identification and control using the Bouc-Wen model*. John Wiley & Sons.

[21] Chen, Y., and Ahmadi, G. (1992) “Wind Effects on Base-Isolated Structures,” *J Eng Mech*, vol. 118, no. 8, pp. 1708–1727, doi: 10.1061/(ASCE)0733-9399(1992)118:8(1708).

[22] Charalampakis, A., and Dimou, C. (2010) “Identification of Bouc–Wen hysteretic systems using particle swarm optimization,” *Computer & Structures*, vol. 88, no. 21–22, pp. 1197–1205.

[23] Kennedy, J., and Eberhart, R. (1995) “Particle swarm optimization,” in *Proceedings of ICNN’95-international conference on neural networks*, pp. 1942–1948.

[24] Millonas, M. (1994) “Swarms, phase transitions, and collective intelligence,” in *Proceeding of Artificial Life*.

[25] Clerc, M., and Kennedy, J., (2002) “The particle swarm-explosion, stability, and convergence in a multidimensional complex space,” *IEEE transactions on Evolutionary Computation*, vol. 6, no. 1, pp. 58–73.

[26] ASCE/SEI 7-22 (2022), *Minimum Design Loads and Associated Criteria for Buildings and Other Structures*. American Society of Civil Engineers. doi: 10.1061/9780784415788.

[27] McKenna, F., Scott, M. H., and Fenves, G. L. (2010) “Nonlinear finite-element analysis software architecture using object composition,” *Journal of Computing in Civil Engineering*, vol. 24, no. 1, pp. 95–107.